THE JOURNAL OF BIOLOGICAL CHEMISTRY
Vol. 270, No. 41, Issue of October 13, pp. 24420–24427, 1995

Printed in U.S.A.

Deficient Geranylgeranylation of Ram/Rab27 in Choroideremia*

(Received for publication, June 27, 1995, and in revised form, August 2, 1995)

Miguel C. Seabra‡, Yiu K. Ho, and Janmeet S. Anant

From the Department of Molecular Genetics, University of Texas Southwestern Medical Center, Dallas, Texas 75235

Choroideremia, an X-linked form of retinal degeneration, results from defects in the Rab escort protein-1 (REP-1) gene. REP-1 and REP-2 assist in the attachment of geranylgeranyl groups to Rab GTPases, a modification essential for their action as molecular switches regulating intracellular vesicular transport. If Rabs that depend preferentially on REP-1 for prenylation exist, they will accumulate unprenylated in choroideremia cells. Using recombinant Rab geranylgeranyl transferase and REPs to label unprenylated cytosolic proteins, we identified one unprenylated protein in choroideremia lymphoblasts that was prenylated *in vitro* more efficiently by REP-1 than by REP-2. This protein was purified and identified as Ram (renamed Rab27), a previously cloned Rab of unknown function. Immunohistochemistry of rat retina showed that Ram/Rab27 is expressed in the pigment epithelium and choriocapillaris, the two retinal cell layers that degenerate earliest in choroideremia. These results raise the possibility that the retinal degeneration in choroideremia results from the deficient geranylgeranylation of Ram/Rab27 or a closely related protein.

Choroideremia (CHM)[1] is a form of X-linked retinal degeneration that can be classified under the broad group of hereditary peripheral retinal dystrophies or retinitis pigmentosa (1). Affected hemizygous males develop slowly progressive retinal degeneration leading to night blindness in their teens, loss of peripheral vision, and complete blindness by middle age. Carrier females generally retain retinal function but exhibit characteristic focal areas of degeneration and pigmentation upon fundoscopic examination, which likely represent clonal areas of disease due to random X inactivation. Pathologic examination of choroideremic eyes show profound atrophy of three adjacent retinal layers, the photoreceptors, the retinal pigment epithelium (RPE), and the choriocapillaris. Studies of carriers and early diseased eyes suggest that the RPE and/or the choriocapillaris are the primary site of degeneration, with secondary involvement of photoreceptors (1). The gene responsible for CHM was localized to chromosomal band Xq21 and isolated by positional cloning techniques (2, 3). An insight into the function of the CHM protein came with the finding that it encodes a subunit of Rab geranylgeranyl transferase, an enzyme that modifies Rab proteins with the covalent attachment of a lipid moiety (4, 5).

Rab proteins are low molecular weight GTPases of the Ras superfamily involved in the regulation of intracellular vesicular traffic in exocytic and endocytic pathways (6–9). More than 30 different Rabs have been identified, each with a characteristic intracellular distribution suggesting that each Rab functions in a distinct transport event, *e.g.* Rab1 functions in endoplasmic reticulum to Golgi transport while Rab5 functions in plasma membrane to endosome transport. A current model for the function of Rab proteins in vesicular transport is based on studies in yeast and mammalian cells. It predicts that Rabs cycle between a cytosolic, inactive, GDP-bound state and a membrane-bound, active, GTP-bound state. The cytosolic form is recruited to the cytoplasmic leaflet of a donor organelle membrane and activated by exchange of the bound GDP for GTP. Once on a transport vesicle, Rabs regulate docking and fusion events that lead to the release of lumenal contents from the transport vesicle into the lumen of the appropriate acceptor organelle. After fusion has occurred, GTP is hydrolyzed to GDP and Rabs are resolubilized by Rab GDP dissociation inhibitor (Rab GDI), which delivers Rabs back to the donor organelle membrane, completing the cycle.

In order for Rabs to interact with intracellular membranes, they must bear C20 geranylgeranyl (GG) groups attached to cysteines at or near the carboxyl terminus of the proteins. Rab proteins that cannot undergo GG modification remain cytosolic and are inactive (10–13). Geranylgeranylation of two carboxyl-terminal cysteines in Rab proteins via thioether bonds is a complex reaction that requires two components (4, 14–16). Rab GG transferase (Rab GGTase, previously designated Component B) or GGTase-II is an α/β heterodimer with structural homology to another prenyl transferase, Ras farnesyl transferase (17). However, unlike farnesyl transferase, Rab GGTase is inactive by itself and requires an accessory protein, designated Rab escort protein (REP, previously designated Component A) that binds to unprenylated Rab, presents it to Rab GGTase, and thereby facilitates GG transfer. After geranylgeranylation, REP remains bound to Rab in a stable complex that can be released *in vitro* by detergents (18). *In vivo*, REP delivers geranylgeranylated Rab to its target donor membrane (19). The structural and functional homology between REP and RabGDI suggests that both use similar mechanisms to deliver Rabs to membranes. It was hypothesized that whereas REP delivers newly synthesized Rabs to target membranes, RabGDI acts in the recycling of Rabs (19).

Peptide sequences derived from purified rat REP-1 and later cDNA cloning revealed that it is the counterpart of the human protein encoded by the CHM gene (4, 18). A partial deficiency of Rab GGTase activity was demonstrated in extracts of CHM-derived lymphoblasts (5). The loss of Rab GGTase activity could be restored by addition of purified REP-1, but not Rab GGTase

* This research was supported by grants from The Foundation Fighting Blindness (National Retinitis Pigmentosa Foundation, Inc.), National Institutes of Health Grant HL20948, and the Perot Family Foundation. The costs of publication of this article were defrayed in part by the payment of page charges. This article must therefore be hereby marked "*advertisement*" in accordance with 18 U.S.C. Section 1734 solely to indicate this fact.

‡ To whom correspondence should be addressed: Dept. of Molecular Genetics, University of Texas Southwestern Medical Center, Dallas, TX 75235. Tel.: 214-648-8643; Fax: 214-648-8804.

[1] The abbreviations used are: CHM, choroideremia; RPE, retinal pigment epithelium, Rab GDI, Rab GDP dissociation inhibitor; GG, geranylgeranyl; GGTase, geranylgeranyl transferase; REP, Rab escort protein; DTT, dithiothreitol; PAGE, polyacrylamide gel electrophoresis; CHAPS, cholamidopropyl-dimethylammonio-propanesulfonate; PBS, phosphate-buffered saline.

(5), consistent with a defective REP-1 gene in CHM. In yeast, both Rab GGTase (encoded by the BET2 and BET4 genes) and REP (encoded by the MRS6/MSI4 gene) activities are essential for cell viability (20–23), and a complete deficiency of REP activity would likely be lethal in humans. The fact that CHM patients have no detectable defect other than the retinal lesion and that CHM cells retain partial Rab GGTase activity suggests that the deficiency of REP-1 is compensated in most tissues of CHM patients. The identification of REP-2 (or CHM-like protein) (24), a protein that is 75% identical to REP-1 (or CHM protein) raised the possibility that REP-2 could compensate for the loss of REP-1 function in CHM. Indeed, recombinant REP-2 can assist in the geranylgeranylation *in vitro* of different Rabs (25).

In search of the molecular mechanisms underlying retinal degeneration in CHM, we hypothesized that the reason why REP-2 is only partially effective in compensating for the loss of REP-1 in CHM retinal cells might be due to the existence of one or more Rabs that depend preferentially on REP-1 for prenylation. In this study, we demonstrate that one Rab protein selectively accumulates unprenylated in the cytosol of CHM lymphoblasts. This protein was purified, sequenced, and identified as the human homolog of a previously identified rat Rab protein, designated Ram (26), which we rename Rab27. Ram/Rab27 is predominantly membrane bound in normal lymphoblasts, whereas it is predominantly cytosolic in CHM lymphoblasts, suggesting that its function is compromised. Furthermore, rat Ram/Rab27 is expressed in normal retinas, specifically in the two cell layers that characteristically degenerate in CHM, the RPE and the choriocapillaris. These results raise the possibility that the retinal degeneration in CHM is due to the defective function of Ram/Rab27 (or a closely related protein) in the RPE and choriocapillaris.

EXPERIMENTAL PROCEDURES

Lymphoblast Cell Lines

Stock cultures of permanent lymphoblast cell lines were grown as described in Seabra *et al.* (5). Briefly, cells were maintained in suspension cultures for 72 h at 37 °C in a 5% CO_2 incubator in RPMI 1640 medium (Sigma) supplemented with 15% heat-inactivated serum, 1 mM sodium pyruvate, penicillin G (100 units/ml), and streptomycin (100 μg/ml). Where indicated, 20 μM compactin in the same medium was added to cells for 6 h before harvesting.

Seven of the nine cell lines used in this study were described previously (5). The cell lines are designated as follows: control cell lines, control-1 (culture designation L389, male, age 38), control-2 (culture L430, male, age 26), control-3 (culture L423, male, age 30), control-4 (culture L429, female, age 24), and control-5 (culture L411, male, age 33); Choroideremia cell lines, CHM-1 (culture L659, male, age 26), CHM-2 (culture L660, male, age 45), CHM-3 (culture L665, male, age 54), and CHM-4 (culture L669, male, age 35). All CHM cell lines contained no detectable REP-1 by immunoblot analysis (data not shown). Large scale production of CHM-1 cells was achieved by growth at 37 °C in 1-liter plastic roller bottles (Falcon) containing RPMI 1640 medium supplemented with glutamax-I (Life Technologies, Inc.), 25 mM sodium HEPES, pH 7.4, and 10% heat-inactivated fetal bovine serum (Life Technologies, Inc.). Initial cultures at a density of 2×10^5 cells/ml were aerated with 10% CO_2, 90% air, and fed every other day with the same medium. Cells at a density of 1×10^6 cells/ml were collected by centrifugation at 1,500 revolutions/min for 15 min at 4 °C, washed once with ice-cold phosphate-buffered saline, recentrifuged as before, and stored frozen at −80 °C.

Assay for Rab Geranylgeranyl Transferase Activity

Rab GGTase activity was determined by measuring the incorporation of [^{3}H]GG pyrophosphate (American Radiolabeled Chemicals, St. Louis, MO) to Rab proteins expressed in *Escherichia coli*, as described previously (5). The standard reaction mixture contained the following components in a final volume of 50 μl: 50 mM sodium HEPES (pH 7.2), 5 mM $MgCl_2$, 1 mM DTT, 1 mM Nonidet P-40, 5.5 μM [^{3}H] GG pyrophosphate (3,000 disintegrations/min/pmol), and the indicated amounts of recombinant Rab proteins, Rab GGTase and REP-1 or REP-2. After incubation for 15 min at 37 °C, the amount of ethanol/HCl precipitable radioactivity was measured by filtration on a glass fiber filter.

The assay to detect unprenylated Rab proteins present in lymphoblasts used the same principle, with the following modifications. Samples to be assayed in a volume of 45 μl were added to reaction mixtures containing 500 mM sodium HEPES (pH 7.2), 50 mM $MgCl_2$, 10 mM DTT, 10 mM Nonidet P-40, 10 μM [^{3}H]GG pyrophosphate (33,000 disintegrations/min/pmol), and 200–800 ng each of Rab GGTase and REP-1 or REP-2 prepared in a volume of 5 μl and incubated for 15 min at 37 °C. The reactions were stopped with the addition of 15 μl of 4 × SDS-sample buffer (27), and aliquots were subjected to SDS-PAGE. Following SDS-PAGE, the gel was either treated with Entensify (DuPont NEN), dried, and exposed to Kodak XAR film at −70 °C or transfered to a nitrocellulose filter and exposed on a PhosphorImager (Fuji). For purification of p27, the same assay containing REP-1, not REP-2, was used.

Purification of p27 from CHM-1 Cells

All steps were carried out at 4 °C.

Steps 1 and 2: Lysis and Ammonium Sulfate Fractionation—Frozen cell pellets (30 ml of packed cells) were thawed and resuspended in 3 volumes of buffer 1 (50 mM Tris-HCl (pH 7.5), 150 mM NaCl, 2 mM $MgCl_2$, 0.5 mM EGTA, 0.5 mM EDTA, 5 mM DTT, 0.1 mM GDP, 0.5 mM phenylmethylsulfonyl fluoride, 5 μg/ml leupeptin, 5 μg/ml pepstatin, and 5 μg/ml aprotinin), and lysed by nitrogen cavitation in a Parr disruption bomb. The lysate was spun at 100,000 × *g* for 1 h, the pellet was discarded, and the supernatant was brought to 40% saturation with solid ammonium sulfate, stirred for 30 min, and centrifuged at 15,000 × *g* for 15 min to remove precipitated proteins. The resulting supernatant was adjusted to 60% saturation with solid ammonium sulfate, and the precipitated material (300 mg of protein) was disolved in one-fifth the initial supernatant volume of buffer 2 (20 mM Tris-HCl (pH 7.5), 150 mM NaCl, 3 mM $MgCl_2$, 1 mM EDTA, 5 mM DTT, and 0.1 mM GDP).

Step 3: Gel Filtration Chromatography—The resuspended material was incubated for 30 min with 10 μg/ml of His-tagged Rab GDI, a generous gift from M. Zerial (EMBL, Heidelberg, Germany) (28) prepared as described below for His-tagged Ram/Rab27. For each run, 3 ml of 40–60% ammonium sulfate fraction (45 mg of protein) was applied onto a Superdex 75 16/60 column (Pharmacia Biotech Inc.) that had been equilibrated in buffer 2. The flow rate was 0.5 ml/min, and the material eluting between 40 and 100 ml was collected in 1-ml fractions. The active fractions were screened by the assay described above and pooled, usually those between 62 and 68 ml of elution.

Steps 4 and 5: Triton X-114 Partitioning and Ion Exchange Chromatography—Triton X-114 partitioning was based on the method of Bordier (29). The active fractions from four gel filtration runs (6 mg of protein) were pooled, adjusted to 1% Triton X-114 (Calbiochem), and incubated for 5 min at 30 °C. The phases were separated by centrifugation at 4,000 revolutions/min for 5 min at 24 °C, the aqueous (upper) phase was collected, adjusted to 2% Triton X-114, and the procedure repeated. The resulting aqueous phase was diluted 1:1 (v/v) in buffer 3 (20 mM Tris-HCl (pH 7.5), 0.1 mM Nonidet P-40, 3 mM $MgCl_2$, 1 mM EDTA, 5 mM DTT, 0.1 mM GDP). The sample (4 mg of protein) was concentrated to 10 ml in Centriprep 10 microconcentrators (Amicon) and loaded onto a Mono Q 5/5 column (Pharmacia) equilibrated in the same buffer. After loading, the column was washed with 10 ml of the same buffer, and the proteins were eluted with a 20-ml linear gradient from 0 to 250 mM NaCl in the same buffer. The flow rate was 1 ml/min, and 2-ml fractions were collected.

Steps 6 and 7: In Vitro Prenylation and Triton X-114 Partitioning—The peak fractions from 10 to 15 Mono Q runs were pooled (0.4–0.6 mg of protein) and concentrated to 1 ml in Centriprep 10 microconcentrators. For *in vitro* prenylation, 150 μl of a reaction mixture containing 333 mM sodium HEPES (pH 7.2), 33.3 mM $MgCl_2$, 6.6 mM DTT, 6.6 mM Nonidet P-40, 5 nmol of [^{3}H]GG pyrophosphate (1,650 distintegrations/min/pmol), 20 μg of Rab GG transferase, and 20 μg of REP-1 was added to the concentrated pool and incubated for 1 h at 37 °C. An aliquot (5%) was taken for determination of the incorporation of [^{3}H]GG into proteins by filter assay, as described above. The remainder was adjusted consecutively to 1% and 4% Triton X-114 and the phases separated as described above. The detergent (bottom) phases were pooled (final volume 200 μl), adjusted to 30 mM Tris-HCl (pH 8.0), 5 mM $MgCl_2$ 1 mM EDTA, and 1.2 ml of ice-cold acetone was added. The mixture was vortexed, incubated for 15 h at −20 °C, and centrifuged in a microfuge for 30 min at 4 °C. The resulting pellet was designated acetone pellet.

Amino Acid Sequence of Peptides from p27

Two strategies were employed to obtain peptides from p27. Method One was designed to isolate and sequence the radiolabeled geranylgeranylated peptide. An estimated 600–700 pmol of [^{3}H]GG groups were incorporated into protein after *in vitro* prenylation, and approximately 90% was recovered in the acetone pellet following Triton X-114 partitioning (see above). The acetone pellet was resuspended in 100 μl of buffer containing 25 mM Tris-HCl (pH 8.0), 4% CHAPS, 1 mM EDTA, after which 15 μg of endoproteinase Lys-C (Boehringer Mannheim) was added and incubated for 18–20 h at 37 °C. When endoproteinase Arg-C (Boehringer Mannheim) was used, the incubation buffer was 100 mM Tris-HCl (pH 7.6), 4% CHAPS, 10 mM $CaCl_2$, 5 mM DTT, 0.5 mM EDTA, and 5 μg of enzyme was added and incubated as above. The resulting peptides were isolated on a reverse-phase μRPC C2/C18 SC 2.1/10 column (Pharmacia) using a SMART System chromatography instrument (Pharmacia). The column was equilibrated in MilliQ water with 0.1% trifluoroacetic acid at 24 °C at a flow rate of 200 μl/min, the samples were injected, and the column eluted with acetonitrile as described in the legend to Fig. 4. Fractions of 100 μl were collected, and an aliquot was counted in a scintillation counter. The peak radioactive fractions were applied directly onto an Applied Biosystems model 470A or 477A Sequencers.

Method Two used a conventional method (30). The sample was subjected to *in vitro* prenylation, Triton X-114 partitioning, and acetone precipitation (approximately 500 pmol of [^{3}H]GG groups incorporated), and then was subjected to electrophoresis on a 12% SDS-PAGE and transferred to nitrocellulose. The nitrocellulose filter was stained with Ponceau S (Sigma) and exposed to a PhosphoImager. The fluorograph was aligned with the nitrocellulose filter, and the corresponding protein band was excised and subjected to solid phase digestion with endoproteinase Lys-C. Peptides released from the filter were purified by high pressure liquid chromatography and sequenced as described previously (4).

cDNA Cloning and E. coli Expression of rat Ram/Rab27

A full-length cDNA encoding rat Ram/Rab27 was obtained by polymerase chain reaction using a 5′ oligonucleotide primer, 5′-GCTCTAGACATATGTCGGATGGAGATTATGACTACCTC-3′, and a 3′ oligonucleotide primer, 5′-TTAAGCTTGGATCCTCAACAGCCGCATAACCCCTTCTC-3′ which were designed on the basis of the rat cDNA sequence (26). An aliquot (1 ng) of rat spleen double-stranded cDNA (QUICK-Clone, Clontech) was used as template for polymerase chain reaction using Pfu DNA polymerase (Stratagene), and the resulting 700-base pair fragment was subcloned into pCR script SK(+) vector (Stratagene). The resulting plasmid was designated pCRS-rRam. A *Nde*I-*Bam*HI fragment from pCRS-rRam, which contained the coding region for rat Ram/Rab27, was ligated into pET14b vector, resulting in the plasmid pET14b-rRab27. Both plasmids were sequenced. The plasmid pET14b-rRab27 encodes a fusion protein that contains six histidine residues at the NH_2 terminus (His-Ram/Rab27). *E. coli* BL21 (DE3) cells were used for protein expression, and the recombinant protein was produced and purified on Ni^{2+}-Sepharose affinity chromatography as described previously (25).

Antibodies, Immunoblotting, and Immunohistochemistry

Antibody N103 is a polyclonal rabbit antibody directed against purified rat His-Ram/Rab27. Rabbits were immunized with 150 μg of His-Ram/Rab27 and immune bleeds collected, as described previously (31). Ten ml of N103 immune serum was applied to 2 ml of a Ram/Rab27 affinity column, prepared by cross-linking 3.5 mg of His-Ram/Rab27 to AminoLink Coupling Gel (Pierce Chemical Co.) as directed by the manufacturer. The column was washed with 20 ml of 10 mM Tris-HCl (pH 7.5), followed by 20 ml of 10 mM Tris-HCl (pH 7.5), containing 0.5 M NaCl. Bound IgG was eluted with 0.1 M glycine (pH 2.9) and collected in 1-ml fractions containing 0.1 ml 1 M Tris-HCl (pH 8.0). N103 antibody was used at concentrations ranging from 0.1 to 1 μg/ml for immunoblot and immunohistochemical analysis. Anti-Rab7 immune sera (a generous gift from M. Zerial, EMBL, Heidelberg, Germany) was diluted 1/1000 for immunoblot and 1/2000 for immunohistochemical analysis. Anti-Rab1 immune sera (a generous gift from B. Goud, Institut Pasteur, Paris, France) was diluted 1/500 for immunoblot analysis. Anti-cellular retinaldehyde binding protein (CRALBP) and anti-opsin immune sera (generous gifts from D. Bok, UCLA) were both diluted 1/2000 for immunohistochemical analysis.

For immunoblot analysis, samples were subjected to SDS-PAGE, transferred to nitrocellulose filters, and stained with 0.2% Ponceau S in 5% acetic acid. The nitrocellulose filters were incubated in solution A (50 mM Tris-HCl (pH 7.4), 150 mM NaCl, 0.2% Tween-20, and 5% nonfat dry milk) for 30 min at room temperature with agitation, followed by incubation in solution 1 containing the primary antibody for 1 h. The blots were washed for 2 × 10 min in solution B (solution A + 1% Nonidet P-40), followed by incubation for 30 min in solution B containing donkey anti-rabbit IgG conjugated to horseradish peroxidase (Amersham Corp.). The blots were then washed for 2 × 10 min with solution C (50 mM Tris-HCl (pH 7.4), 1% SDS, 0.5% cholic acid, and 1% Nonidet P-40). Bound IgG was visualized by the ECL method (Amersham). All blots were calibrated with prestained molecular weight markers (Bio-Rad).

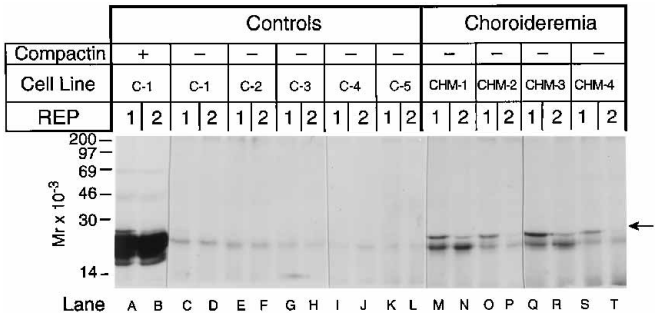

FIG. 1. **REP-dependent transfer of [^{3}H]geranylgeranyl to lymphoblast proteins.** Cytosolic extracts were prepared as described under "Experimental Procedures" in buffer containing 20 mM sodium HEPES (pH 7.2), 10 mM NaCl, 0.1 mM Nonidet P-40, and 1 mM DTT, from human normal lymphoblasts (*controls*, *lanes A-L*) or choroideremia lymphoblasts (*CHM*, *lanes M-T*) grown in the presence (+) or absence (−) of compactin as indicated. Extracts (50 μg for *lanes A* and *B* and 125 μg for *lanes C-T*) were subjected to *in vitro* prenylation, in the presence of 1 μM [^{3}H]GG pyrophosphate, 200 ng of Rab GG transferase, and 800 ng of either REP-1 or REP-2 as indicated. Reaction mixtures were stopped after 30 min at 37 °C with SDS-sample buffer, subjected to SDS-PAGE on 10–20% precast minigels (Bio-Rad), the gel was enhanced with Entensify (DuPont NEN) and exposed to Kodak XAR film for 14 days at −70 °C. Gels were calibrated with the indicated molecular weight standards. *Arrow* at *right* denotes the position of migration of p27.

For immunohistochemistry, Sprague-Dawley rats were perfused with phosphate-buffered saline (PBS) (pH 7.4) prior to dissection of the eye cup, which included the retina, pigment epithelium, choroid, and sclera. The tissue was immediately placed in 4% paraformaldehyde in PBS (pH 7.4) for 12 h at 4 °C. The tissue was infiltrated with 30% (w/v) sucrose in PBS (pH 7.4) at 4 °C, embedded in O.C.T compound (Tissue-Tek), and frozen in this media on dry ice. Longitudinal frozen sections (10–12 μm) of the eye cup were placed on Superfrost/Plus microscope slides (Fisher). Immunohistochemical staining of these sections was performed using the Vectastain ABC Elite kit following the instructions of the manufacturer (Vector Laboratories). Normal goat serum (1.5%) was added to the incubation solution (PBS (pH 7.4) and 0.3% Triton X-100) during incubation of tissue sections with IgG and avidin-biotin complexes. Bound antibodies were detected using an alkaline phosphatase substrate (Vector Laboratories Alkaline Phosphatase Substrate Kit III), resulting in a blue colorimetric reaction. Competition of N103 antibody immunostaining was performed by incubation of diluted N103 antibody (0.5 μg/ml) with AminoLink Coupling Gel (Pierce) beads cross-linked with 10 × molar excess of either His-Ram/Rab27 or His-Rab1a prepared as described above, at 22 °C with agitation for 1 h. The beads were then sedimented by centrifugation, and the resulting supernatant was utilized for immunohistochemistry.

Subcellular Distribution of Ram/Rab27

Cytosolic and membrane fractions from cultured lymphoblast cell lines and rat tissues were prepared as follows. The cells or tissues were homogenized thoroughly in 3 volumes of buffer 1. The homogenate was centrifuged at 800 × *g* at 4 °C to sediment unbroken cells and cell nuclei. The postnuclear supernatant was then centrifuged at 100,000 × *g* for 1 h at 4 °C, resulting in the separation of cytosolic (supernatant) and membrane (pellet) fractions. The pellet was resuspended in buffer 1 adjusted to 1% Nonidet P-40. The protein content of cytosolic and 1% Nonidet P-40-solubilized membrane fractions was determined using the Coomassie Plus Protein Assay Reagent (Pierce).

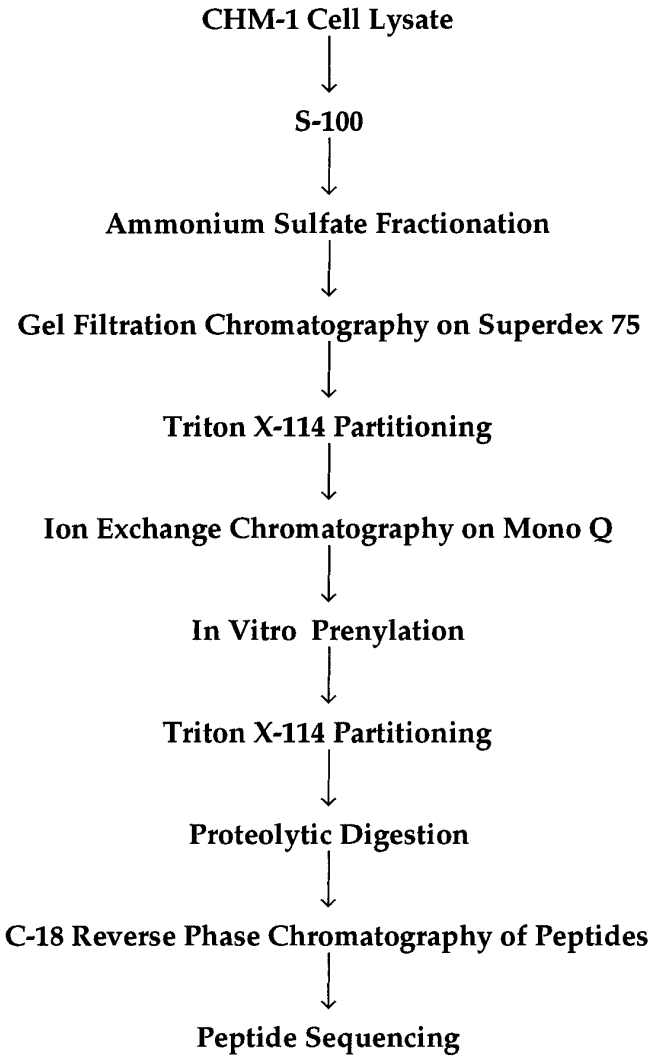

FIG. 2. **Purification scheme for p27.** Details are described under "Experimental Procedures" and "Results."

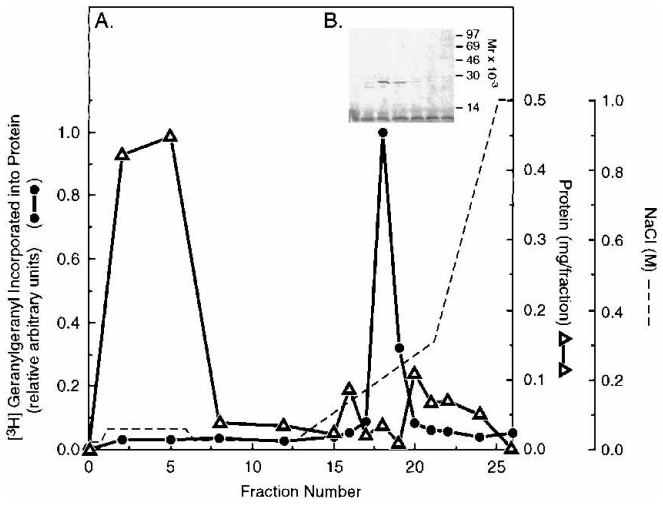

FIG. 3. **Purification of p27 by Mono Q chromatography.** (*A*), the aqueous phase from Triton X-114 partitioning was processed as described under "Experimental Procedures" and applied onto a Mono Q 5/5 column equilibrated in buffer 3 (*fractions 1–5*). The column was washed with 10 ml in the same buffer (*fractions 6–10*), and proteins were eluted with two sequential linear gradients, a 20-ml gradient from 0 to 250 mM NaCl (*fractions 11–20*), followed by 5 ml of a gradient from 250 mM to 1 M NaCl (*fractions 21–23*) in the same buffer, and then washed for 5 ml with 1 M NaCl in the same buffer (*fractions 24–26*). The amount of protein present in each fraction was determined by the method of Bradford (△). An aliquot (45 μl) of each fraction was assayed for incorporation of [^{3}H]geranylgeranyl into proteins (●) by *in vitro* prenylation, as described under "Experimental Procedures". Assayed fractions were separated on 12.5% SDS-polyacrylamide gel, transferred to nitrocellulose, and exposed for 15 h using a Fuji PhosphorImager. The units obtained from the digital imager are arbitrary and plotted relative to the maximum value in fraction 17 (assigned a value of 1.0). (*B*), the *inset* shows the actual image obtained to deduce these values. Only fractions 16–22 are shown. The gel was calibrated with the indicated ^{14}C-methylated protein standards.

RESULTS

To determine if CHM lymphoblasts efficiently prenylate all their cellular Rabs *in vivo*, we prepared cytosolic extracts from CHM and normal lymphoblasts and subjected them to *in vitro* prenylation using [^{3}H]GG pyrophosphate as the lipid donor, Rab GGTase, and either REP-1 or REP-2. Under these conditions, any unprenylated Rab present in the cytosolic extract will be covalently modified by [^{3}H]GG groups and may be detected upon SDS-PAGE and autoradiography. When five different normal extracts were analyzed in this manner, virtually no radiolabeled proteins were detected (Fig. 1, *lanes C-L*), suggesting that newly synthesized Rabs are rapidly and efficiently prenylated in normal cells. When the same cells were grown in the presence of compactin, an inhibitor of the synthesis of mevalonate, the precursor of prenyl groups, a large number of cytosolic proteins with apparent molecular mass between 20 and 30 kDa were labeled (Fig. 1, *lanes A* and *B*), indicating that unprenylated endogenous Rabs can be detected using this method. A similar pattern of bands was obtained when using either recombinant REP-1 or REP-2, consistent with the idea that either REP-1 or REP-2 can efficiently process most Rabs *in vitro* (25).

When extracts from four different CHM cell lines were subjected to *in vitro* prenylation, a strikingly different result was obtained. Two discrete bands of approximately 27 and 23 kDa were radiolabeled in all four CHM-derived extracts (Fig. 1, *lanes M-T*). The 27 kDa band appears to be labeled by REP-1, but not REP-2 (Fig. 1, compare *lanes M* and *N*), while the 23 kDa band appears equally intense when using either REP. This pattern of labeling is characteristic of all CHM extracts (Fig. 1, *lanes M-T*). As a control, we subjected extracts derived from patients with Usher Syndrome type II (5), another disease leading to retinal degeneration, to the same procedure and observed that no proteins could be labeled, as observed for normal cells (data not shown). The 27 kDa band therefore meets the criteria for a protein that is preferentially processed by REP-1 both *in vitro* and *in vivo*. The 27-kDa protein is the only major protein observed upon two-dimensional SDS-PAGE (data not shown). The 23-kDa band is not a single band; it represents the sum of many faint bands, as could be demonstrated upon subsequent purification. They might represent a small fraction of other Rabs that accumulate unprenylated in CHM cells due to slower prenylation kinetics when REP-1 is missing.

We devised a purification scheme in order to isolate and identify the 27-kDa unprenylated protein (p27) (Fig. 2). All fractions were subjected to *in vitro* prenylation with [^{3}H]GG pyrophosphate to detect p27. We obtained a cytosolic soluble fraction (S-100) from CHM-1 cells, discarding the membranes that contain the majority of prenylated Rabs, and subjected the S-100 fraction to ammonium sulfate fractionation. The 40–60% ammonium sulfate fraction was incubated with an excess of recombinant Rab GDI prior to gel filtration chromatography. Since only prenylated Rabs form an 80-kDa complex with Rab GDI (8), the rationale for this step was to separate unprenylated p27 from other prenylated Rabs present in the ammo-

nium sulfate fraction. As predicted, p27 eluted from the column at approximately 30 kDa, the behavior of a monomer (data not shown). The fractions containing p27 were subjected to Triton X-114 partitioning where p27 partitioned into the aqueous phase as predicted for an unprenylated hydrophilic protein. We then subjected the Triton X-114 aqueous phase to ion-exchange chromatography on a Mono Q column (Fig. 3). p27 eluted at about 200 mM NaCl. When this fraction was prenylated *in vitro*, p27 was the only protein that was labeled (Fig. 3, *inset*).

We then took advantage of the fact that we could render p27 both radiolabeled and hydrophobic by prenylating it *in vitro* with [^{3}H]GG pyrophosphate. Therefore, we performed a bulk prenylation of the p27-containing fractions from the Mono Q column. The [^{3}H]GG-p27 was again subjected to Triton X-114 partitioning and the majority of [^{3}H]GG-p27 now partitioned into the detergent phase as predicted (data not shown). This step resulted in a very significant purification, since most proteins remained in the aqueous phase. The fraction contained only about 15–20 proteins of different molecular weights as visualized by gold staining of a nitrocellulose filter, following SDS-polyacrylamide gel electrophoresis, and transfer.

In order to identify the 27-kDa protein, we digested the protein *in vitro* with proteases, and then we isolated and sequenced the [^{3}H]GG-radiolabeled peptide. This prenylated peptide is considerably more hydrophobic than non-modified peptides and was eluted after all other peptides upon C-18 reverse phase chromatography. Fig. 4 shows the profile obtained upon C-18 reverse phase chromatography of a sample digested with either endoproteinase Lys-C (*panel A*) or endoproteinase Arg-C (*panel B*). The peak fractions in experiment A eluted between 5.75 and 5.95 ml. They contained 360 pmol of peptide which accounted for 75% of radiolabel incorporated into starting material (fractions 23–24). In experiment B, the peak fractions eluted between 4.85 and 5.25 ml and contained 250 pmol of peptide or 41% of the starting material (fractions 14–17). Peptide sequences were obtained (Table I, peptides 1 and 2) and compared with sequences in a protein data bank (Swiss-Prot, September 1994). We observed a close match to the predicted sequence of a rat protein designated Ram (26). Ram is a mem-

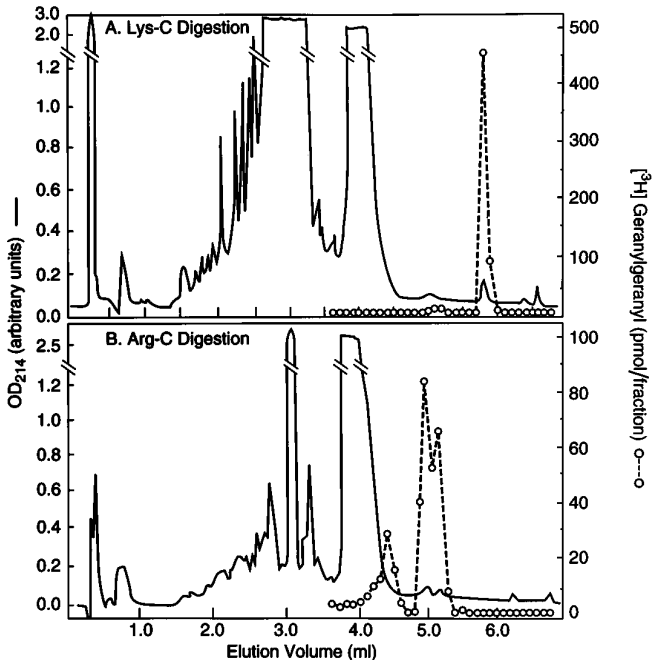

FIG. 4. **Isolation of peptides from p27 by C-18 reverse phase chromatography.** p27 was radiolabeled with [^{3}H]geranylgeranyl by *in vitro* prenylation, followed by Triton X-114 partitioning and acetone precipitation as described under "Experimental Procedures." The protein pellet was incubated with either endoproteinase Lys-C (*panel A*) or Arg-C (*panel B*), and the resulting peptides were isolated on a reverse-phase μRPC column using a SMART® System chromatography instrument. The column was equilibrated in MiliQ water with 0.1% trifluoroacetic acid at 24 °C at a flow rate of 200 μl/min, the samples were injected, and the column was washed with 1 ml of the same solution. The peptides were eluted with a 3.5-ml linear gradient between 0 and 70% acetonitrile with 0.1% trifluoroacetic acid, followed by a 2.5-ml linear gradient between 70 and 100% of the same solution. One-hundred μl fractions were collected after 3.5 ml of elution, and an aliquot was counted in a scintillation counter (○). The absorbance detected at 214 nm is shown as a *straight line*.

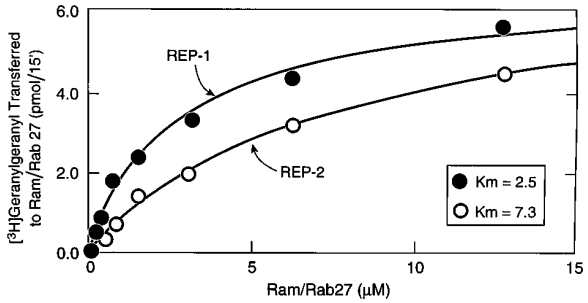

FIG. 5. **Geranylgeranylation of Ram/Rab27 by REP-1 or REP-2.** Each reaction mixture contained, in a final volume of 50 μl, 5.5 μM [^{3}H]GG pyrophosphate, 50 ng of Rab GGTase, 50 ng of either REP-1 (●) or REP-2 (○), and the indicated concentrations of Ram/Rab27. After incubation for 15 min at 37 °C, the amount of [^{3}H]GG transfered to Ram/Rab27 was measured by ethanol/HCl precipitation. The value obtained in the absence of Ram/Rab27 was 0.11 pmol. Each value represents the average of duplicate reactions. The apparent K_m values obtained using k·cat software are indicated. The standard errors for the mean were ± 0.4 for REP-1 and ± 0.8 for REP-2.

TABLE I

Sequence of peptides from purified human p27: comparison with amino acid sequence of rat Ram/Rab27

The sequences derived from human p27 were obtained from peptides isolated as described under "Experimental Procedures" and Fig. 4. Question marks refer to unidentified or ambiguous residues. Residues in parentheses refer to inferred basic amino acid present NH_2-terminal to the endoproteinase cleavage site, K for endoproteinase Lys-C, or R for endoproteinase Arg-C. Nonidentical residues between the human and rat sequences are underlined. Rat Ram/Rab27 sequence was obtained from Nagata *et al.* (26).

Peptide No.	Origin of peptide	Amino acid sequence	Residue in cDNA sequence
1	Human p27	(R)SNGHASTDQLSEEK?K?A	
	Rat Ram/Rab27	R SNGHTSTDQLSEEKEKGL	200–218
2	Human p27	(K)GA?G?	
	Rat Ram/Rab27	K GLCGC	216–221
3	Human p27	(K)FLALGDSGVGK	
	Rat Ram/Rab27	K FLALGDSGVGK	11–22
4	Human p27	(K)TSVLYQYTDGK	
	Rat Ram/Rab27	K TSVLYQYTDGK	22–33

ber of the Rab family of low molecular weight GTPases, and for the remainder of the text we will refer to it as Ram/Rab27 (see below "Discussion"). In later experiments, when larger amounts of p27 were purified, we confirmed its identity as Ram/Rab27 by proteolytic digestion of the protein and isolation of two internal peptides using standard methods (30). The sequenced peptides showed a 100% match with rat Ram over 22 amino acids (Table I, peptides 3 and 4).

We isolated a cDNA encoding Ram/Rab27 from rat spleen cDNA by polymerase chain reaction and prepared a hexahistidine-tagged version of recombinant Ram/Rab27 by expression in *E. coli* and purification by nickel-Sepharose chromatography. Kinetic analysis of recombinant Ram/Rab27 in prenylation reactions using REP-1 or REP-2 revealed that the maximal reaction velocity was approximately the same when either REP was used in the reaction, but there was a 3-fold higher apparent K_m with REP-2 as compared with REP-1 (Fig. 5). In other experiments, we compared directly the prenylation kinetics of Rab1a, Rab3a, and Ram/Rab27 (Table II). As previously reported by Cremers *et al.* (25), we observed similar K_m and V_{max} values for REP-1 and REP-2 when Rab1a was the substrate, and a similar K_m but 3-fold lower V_{max} for REP-2 when Rab3a was the substrate. In the same experiments, we obtained a similar V_{max} for REP-1 and REP-2 but 2–3-fold higher K_m for REP-2 when Ram/Rab27 was the substrate, comparable to the values obtained in Fig. 5. We observed the same result in three independent experiments using different batches of REP-1 and REP-2.

We obtained two different polyclonal antibodies against rat Ram/Rab27, one directed against a COOH-terminal peptide and the other against the entire recombinant protein. The antibodies were highly specific and reacted against the rat protein with high affinity. They also detected the human counterpart, albeit with lower affinity. Despite the presence of some nonspecific bands, we were able to study the distribution of Ram/Rab27 in human lymphoblasts from the same subjects shown in Fig. 1. In all of the normal cell lines, Ram/Rab27 was present exclusively in the membrane fraction (Fig. 6, *lanes A-J*). A different result was obtained in all four CHM cell lines studied. In these cells, Ram/Rab27 was significantly shifted to the cytosol and only 20–30% remained in the membrane fraction (Fig. 6, *lanes K-R*). Similar results were obtained with both anti-Ram/Rab27 antibodies. There were only slight changes, if any, in distribution between normal and CHM cells for other Rabs, such as Rab1 or Rab7 (Fig. 6). These data confirm that the prenylation defect in CHM cells affects specifically Ram/Rab27.

To determine whether Ram/Rab27 is expressed in the retina, we used the anti-Ram/Rab27 antibody produced against the recombinant protein to probe membrane extracts derived from various rat tissues. Ram/Rab27 was present at high levels in eye, intestine, lung, pancreas, and spleen, and low or absent in brain, liver, heart, kidney, and skeletal muscle (Fig. 7). The high affinity and the specificity of this antibody allowed more detailed studies of the rat retina by immunohistochemistry. As shown in Fig. 8*A*, the anti-Ram/Rab27 antibody stained strongly the retinal pigment epithelium (*RPE*) and the choriocapillaris. This staining was competed with Ram/Rab27 protein (Fig. 8*B*) but not with Rab1a protein (Fig. 8*C*), suggesting that it is specific. Another antibody directed against the COOH terminus of Ram/Rab27 gave identical results (data not shown). Specific staining of other retinal layers was obtained when we used an anti-Rab7 antibody that stains the RPE and plexiform layers but not the choriocapillaris (Fig. 8*D*), an anticellular retinaldehyde-binding protein that stains the RPE (Fig. 8*E*) and an anti-opsin antibody that stains the rod outer segments (Fig. 8*F*). In each case, the staining pattern was different from that of Ram/Rab27.

DISCUSSION

We previously proposed that in CHM cells where REP-1 is missing, REP-2 can assist in the prenylation of most Rabs

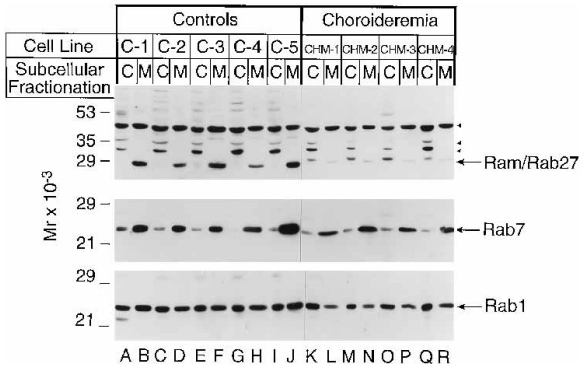

FIG. 6. **Subcellular distribution of Rabs in control and choroideremia lymphoblasts.** Cytosolic (*C*) and membrane (*M*) fractions were prepared as described under "Experimental Procedures" from human normal lymphoblasts (*controls*, *lanes A-J*) or choroideremia lymphoblasts (*lanes K-R*). Extracts (25 μg each) were subjected to SDS-PAGE on 12.5% acrylamide gels, the proteins transferred to nitrocellulose filters, and Rabs were detected by immunoblot analysis, as described under "Experimental Procedures." Anti-Ram/Rab27 affinity-purified N103 antibody was used at 1 μg/ml. *Arrows* at *right* denote the position of migration of Ram/Rab27, Rab7, and Rab1, as indicated. *Arrowheads* at *right* denote cross-reacting bands revealed by the anti-Ram/Rab27 antibody. Gels were calibrated with the indicated molecular weight standards.

TABLE II

Kinetics of geranylgeranylation of Rab proteins: comparison between REP-1 and REP-2

Geranylgeranylation of Rab proteins was determined under standard conditions in the presence of 50–100 ng of Rab GG transferase and 50–100 ng of either REP-1 or REP-2, as described under "Experimental Procedures." Kinetic parameters were analyzed with the software k·cat (Biometallics, Princeton, NJ) on a Macintosh computer. The program was used to calculate the substrate concentration giving half-maximal velocity (apparent K_m) and the maximal velocity (apparent V_{max}). The standard errors of the mean are indicated. These values were determined from substrate saturation curves ranging from 0.1 to 20 μM. Experiments A and B refer to two independent experiments performed with different batches of *REP-1* and *REP-2*.

REP	Rab	Apparent K_m		Apparent V_{max}	
		Exp. A	Exp. B	Exp. A	Exp. B
		μM		*nmol·min^{-1}·mg of protein^{-1}*	
REP-1	Rab1a	2.3 ± 0.7	2.0 ± 0.3	15.5 ± 1.7	14.5 ± 0.5
REP-2	Rab1a	2.6 ± 0.6	1.7 ± 0.2	16.9 ± 1.4	14.7 ± 0.4
REP-1	Rab3a	2.2 ± 0.2	2.1 ± 0.3	4.3 ± 0.2	4.9 ± 0.2
REP-2	Rab3a	2.0 ± 0.3	3.0 ± 0.2	1.5 ± 0.1	2.0 ± 0.04
REP-1	Ram/Rab27	2.5 ± 0.3	2.6 ± 0.2	8.5 ± 0.3	8.4 ± 0.2
REP-2	Ram/Rab27	5.7 ± 0.8	5.6 ± 0.9	9.1 ± 0.6	9.6 ± 0.6

thereby compensating for the loss of REP-1 and preventing overt cellular dysfunction (5, 25). The question remained: why does the retina degenerate? The current data provide a potential explanation. We have found that CHM lymphoblasts efficiently prenylate the majority of its Rab proteins, except for one protein that accumulates unprenylated. This protein, Ram/Rab27, is expressed at high levels in the retinal pigment epithelium and choriocapillaris, the two sites of earliest degeneration in CHM.

We demonstrate that CHM lymphoblasts contain one protein that requires preferentially REP-1 for prenylation both *in vivo* and *in vitro*. We isolated the REP-1-dependent substrate and identified it by peptide sequencing as the human homolog of a rat protein previously cloned by Nagata *et al.* (26) and designated Ram. These investigators studied GTP-binding proteins present in human platelets and purified a protein designated c25KG (32). Using peptide sequences obtained from c25KG, they cloned a related but not identical gene from a rat megakaryocyte library, Ram (26). Ram is a member of the Ras superfamily of GTPases. It shows less than 30% identity with members of the Ras, Rho/Rac, Arf, and Ran families and more than 30% identity with members of the Rab family (26). Ram contains a carboxyl-terminal prenylation motif, CysGlyCys and an effector domain characteristic of Rab proteins. For these reasons we propose to rename it Rab27, in accordance with widely accepted nomenclature rules (33). Ram/Rab27 is more closely related to Rab3 (40% identical) than to any other subfamily of Rabs, but the level of identity suggests that Ram/Rab27 represents a distinct subfamily (which may include c25KG). No clues exist to date as to the physiological role of Ram/Rab27, except to speculate that it is regulating one step of intracellular vesicular transport, as proposed for other better studied Rabs.

We raised specific antibodies directed against Ram/Rab27 and demonstrate that it has a different subcellular distribution in normal *versus* CHM lymphoblasts. In normal lymphoblasts the protein is mostly membrane bound, but in CHM cells Ram/Rab27 is predominantly cytosolic. Two other Rabs studied show similar distribution in both normal and CHM lymphoblasts. These findings support the conclusion that the correct protein was identified insofar as it has been extensively documented that Rabs require prenyl groups for membrane attachment and that they become cytosolic and inactive in their absence (see Introduction).

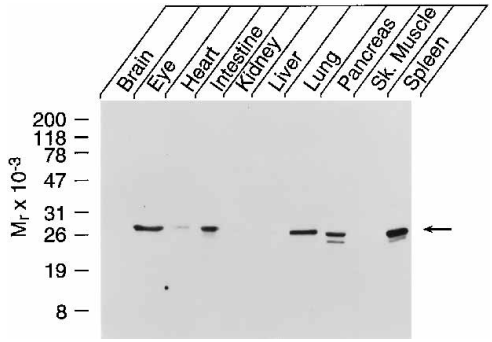

FIG. 7. **Tissue distribution of rat Ram/Rab27 as determined by immunoblot analysis.** Membrane fractions of the indicated rat tissues were prepared as described under "Experimental Procedures," and subjected (50 μg each) to SDS-PAGE on 12.5% acrylamide gels. The proteins were transferred to nitrocellulose filters and stained by Ponceau S to verify that equal amounts of proteins were loaded in each lane. Ram/Rab 27 was detected by immunoblot analysis using 0.1 μg/ml affinity-purified N103 antibody as described under "Experimental Procedures." *Arrow* at *right* denotes the position of migration of Ram/Rab27. Gels were calibrated with the indicated molecular weight standards.

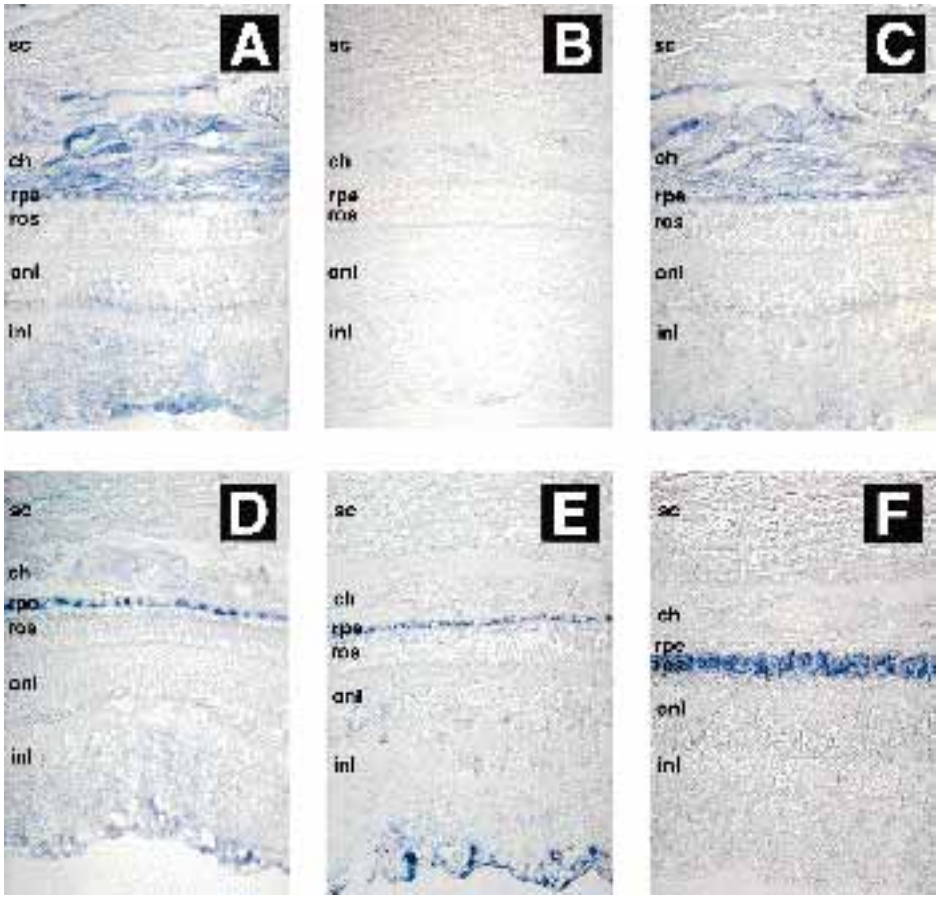

FIG. 8. **Immunohistochemical localization of Ram/Rab27 in the rat retina.** Longitudinal frozen rat retina sections (10 μm) were prepared and immunostained with 0.5 μg/ml of affinity-purified anti-Ram/Rab27 N103 antibody (*A*), 0.5 μg/ml of affinity-purified anti-Ram/Rab27 N103 antibody in the presence of 10 $\times$ molar excess of His-Ram/Rab27 (*B*) or His-Rab1A (*C*), anti-Rab7 immune sera (*D*), anti-cellular retinaldehyde-binding protein antibody immune sera (*E*), and anti-opsin immune sera (*F*), as described under "Experimental Procedures." The abbreviations used are: *sc*, sclera; *ch*, choroid; *rpe*, retinal pigment epithelium; *ros*, rod photoreceptor outer segments; *onl*, outer nuclear layer; *inl*, inner nuclear layer.

When we analyzed the kinetics of *in vitro* prenylation of Ram/Rab27, we observed a 2–3-fold higher apparent K_m in the reaction when REP-2 was present as compared with REP-1. This finding suggests that there is lower affinity for the REP-2-Ram/Rab27 interaction, as compared to REP-1-Ram/Rab27. We think that this change in apparent K_m is significant and suggests a mechanism for its deficient prenylation in CHM cells. We previously analyzed different recombinant Rabs (Rab1a, Rab3a, Rab3b, Rab3d, Rab5a, and Rab6) and were never able to demonstrate a change in the apparent K_m of the reaction, either between different Rabs or the same Rab toward REP-1 and REP-2 (25). Since all other Rabs tested show higher affinity for REP-2 than Ram/Rab27, it is possible that Ram/Rab27 cannot compete efficiently with other Rabs for prenylation in CHM cells where REP-1 is missing. By this formulation, the deficient prenylation of Ram/Rab27 in CHM cells would result in its inactivation and subcellular redistribution from the membrane into the cytosol and is entirely consistent with the data presented here.

We demonstrate here that Ram/Rab27 is present in the retina, namely in the two cell layers believed to degenerate primarily in CHM, the RPE and the choriocapillaris. The photoreceptors did not show significant expression of Ram/Rab27. Labeling of the RPE and the choriocapillaris layers was intense, reproduced with two different antibodies, and competed by soluble Ram/Rab27 protein but not by the related protein Rab1a, which suggest that the staining was specific.

Taken together, these results suggest a mechanism for the retinal degeneration in CHM. Ram/Rab27 is postulated to play an important and unique role in the regulation of a specific vesicular transport step in RPE and/or choriocapillaris cells. The inability to efficiently prenylate Ram/Rab27 in these cells leads to a functional defect that ultimately results in cellular death. The dysfunction of the RPE/choriocapillaris results in the secondary degeneration of photoreceptors and visual impairment. The slow progression of the disease may be explained by the fact that not all Ram/Rab27 is unprenylated and that a fraction is membrane bound and presumably fully functional. With age, these cells may become more sensitive to the functional loss of Ram/Rab27 and degenerate.

Why is CHM confined to the retina if Ram/Rab27 is expressed in other tissues? It is possible that in other tissues, Ram/Rab27 function is redundant and compensated by a related Rab (such as c25KG); alternatively, enough function may be provided by the remainder of active Ram/Rab27, or the dysfunctional transport step may not be so crucial to the viability of those tissues. Another possibility is that in the retina there is a more severe defect in geranylgeranylation of Ram/Rab27, either because there is less REP-2 present or because there are more competitor Rabs to be prenylated.

We have not yet ruled out that the crucial Rab that is not prenylated in CHM retinas is a protein related to Ram/Rab27 and not Ram/Rab27 itself. As discussed above, there is at least one related protein, c25KG and others may exist. Also, it remains to be shown that human retinas express Ram/Rab27 in the same cell types and that the findings in the rat are relevant to the human disease. These and other issues may be addressed with future studies detailing the function of Ram/Rab27 and related proteins in the RPE, the choriocapillaris, and other tissues.

Acknowledgments—We thank Mike Brown and Joe Goldstein for support, many helpful suggestions, and critical reading of the manuscript, Susan Burke, Robin Craddock, and Ann Rickert for excellent technical assistance, Emily Hunter for help with purification of p27, Clive Slaughter for sequencing, Laura Deane, Ravi Pathak, and Joachim Herz for help with immunohistochemistry, and Marino Zerial, Bruno Goud, and Dean Bok for antibodies.

REFERENCES

1. Heckenlively, J. R., and Bird, A. C. (1988) *Retinitis Pigmentosa* (Heckenlivelys, J. R., eds) pp. 176–187, J. B. Lippincott Co., New York
2. Cremers, F. P., van de Pol, D. J., van Kerkhoff, L. P., Wieringa, B., and Ropers, H. H. (1990) *Nature* **347,** 674–677
3. Merry, D. E., Janne, P. A., Landers, J. E., Lewis, R. A., and Nussbaum, R. L. (1992) *Proc. Natl. Acad. Sci. U. S. A.* **89,** 2135–2139
4. Seabra, M. C., Brown, M. S., Slaughter, C. A., Sudhof, T. C., and Goldstein, J. L. (1992) *Cell* **70,** 1049–1057
5. Seabra, M. C., Brown, M. S., and Goldstein, J. L. (1993) *Science* **259,** 377–381
6. Simons, K., and Zerial, M. (1993) *Neuron* **11,** 789–799
7. Pfeffer, S. R. (1994) *Curr. Opin. Cell Biol.* **6,** 522–526
8. Nuoffer, C., and Balch, W. E. (1994) *Annu. Rev. Biochem.* **63,** 949–990
9. Novick, P. J., and Brennwald, P. (1993) *Cell.* **75,** 597–601
10. Walworth, N. C., Goud, B., Kabcenell, A. K., and Novick, P. J. (1989) *EMBO J.* **8,** 1685–1693
11. Kinsella, B. T., and Maltese, W. A. (1991) *J. Biol. Chem.* **266,** 8540–8544
12. Gorvel, J. P., Chavrier, P., Zerial, M., and Gruenberg, J. (1991) *Cell* **64,** 915–925
13. Lombardi, D., Soldati, T., Riederer, M. A., Goda, Y., Zerial, M., and Pfeffer, S. R. (1993) *EMBO J.* **12,** 677–682
14. Brown, M. S., and Goldstein, J. L. (1993) *Nature* **366,** 14–15
15. Farnsworth, C. C., Seabra, M. C., Ericsson, L. H., Gelb, M. H., and Glomset, J. A. (1994) *Proc. Natl. Acad. Sci. U. S. A.* **91,** 11963–11967
16. Seabra, M. C., Goldstein, J. L., Sudhof, T. C., and Brown, M. S. (1992) *J. Biol. Chem.* **267,** 14497–14503
17. Armstrong, S. A., Seabra, M. C., Sudhof, T. C., Goldstein, J. L., and Brown, M. S. (1993) *J. Biol. Chem.* **268,** 12221–12229
18. Andres, D. A., Seabra, M. C., Brown, M. S., Armstrong, S. A., Smeland, T. E., Cremers, F. P. M., and Goldstein, J. L. (1993) *Cell* **73,** 1091–1099
19. Alexandrov, K., Horiuchi, H., Steele, M. O., Seabra, M. C., and Zerial, M. (1994) *EMBO J.* **13,** 5262–5273
20. Waldherr, M., Ragnini, A., Schweyer, R. J., and Boguski, M. S. (1993) *Nature Genet.* **3,** 193–194
21. Fujimura, K., Tanaka, K., Nakano, A., and Toh-e, A. (1994) *J. Biol. Chem.* **269,** 9205–9212
22. Jiang, Y., Rossi, G., and Ferro-Novick, S. (1993) *Nature* **366,** 84–86
23. Jiang, Y., and Ferro-Novick, S. (1994) *Proc. Natl. Acad. Sci. U. S. A.* **91,** 4377–4381
24. Cremers, F. P., Molloy, C. M., van de Pol, D. J., van den Hurk, J. A., Bach, I., Geurts van Kessel, A. H., and Ropers, H. H. (1992) *Hum. Mol. Genet.* **1,** 71–75
25. Cremers, F. P., Armstrong, S. A., Seabra, M. C., Brown, M. S., and Goldstein, J. L. (1994) *J. Biol. Chem.* **269,** 2111–2117
26. Nagata, K., Satoh, T., Itoh, H., Kozasa, T., Okano, Y., Doi, T., Kaziro, Y., and Nozawa, Y. (1990) *FEBS Lett.* **275,** 29–32
27. Laemmli, U. K. (1970) *Nature* **227,** 680–685
28. Huber, L. A., Ullrich, O., Takai, Y., Lutcke, A., Dupree, P., Olkkonen, V., Virta, H., de Hoop, M. J., Alexandrov, K., Peter, M., Zerial, M., and Simons, K. (1994) *Proc. Natl. Acad. Sci. U. S. A.* **91,** 7874–7878
29. Bordier, C. (1981) *J. Biol. Chem.* **256,** 1604–1607
30. Fernandez, J., DeMott, M., Atherton, D., and Mische, S. M. (1992) *Anal. Biochem.* **201,** 255–264
31. Reiss, Y., Seabra, M. C., Armstrong, S. A., Slaughter, C. A., Goldstein, J. L., and Brown, M. S. (1991) *J. Biol. Chem.* **266,** 10672–10677
32. Nagata, K., Itoh, H., Katada, T., Takenaka, K., Ui, M., Kaziro, Y., and Nozawa, Y. (1989) *J. Biol. Chem.* **264,** 17000–17005
33. Kahn, R. A., Der, C. J., and Bokoch, G. M. (1992) *FASEB J.* **6,** 2512–2513